



345 E. 47th St., New York, N.Y. 10017

The Society shall not be responsible for statements or opinions advanced in papers or discussion at meetings of the Society or of its Divisions or Sections, or printed in its publications. Discussion is printed only if the paper is published in an ASME Journal. Papers are available from ASME for 15 months after the meeting.

Printed in U.S.A.

Copyright © 1993 by ASME

SWIRL GENERATION AND RECIRCULATION USING RADIAL SWIRL VANES

John L. Halpin

Advanced Engine Engineering Division
G.E. Aircraft Engines
Cincinnati, Ohio

ABSTRACT

The concept of the Swirl Number and its effect on recirculation is reviewed and problems with it are identified. Swirl generation through the use of radial inlet swirl vanes is then studied. The effect of vane and swirl cup design on recirculation is then evaluated using finite element computer modeling and verified using tufting tests. Vane geometry, combustor dome geometry, co- vs. counter-rotation and mass flow effects are all evaluated. It is shown that co- and counter-rotation generate very similar flow fields and recirculated mass flows. An approach for calculating swirl numbers in multiple swirler designs is proposed.

NOMENCLATURE

B_p	vane-to-vane throttling gap (ball gap)
C	center point in radial swirler geometry
G_x	axial flux of axial momentum (lbs)
G_t	axial flux of tangential momentum (ft. • lbs)
L_{rz}	length of the recirculation zone (in)
p	static pressure (psi or psf)
P_{Tin}	total pressure at the inlet (psia)
P_{Sout}	static pressure at the exit (psia)
r	a radius (ft)
R	swirler exit radius (ft)
R_d	combustor dome height or can diameter (ft or in)
R_i	inner radius of the swirl vanes (ft)
R_o	outer radius of the swirl vanes (ft)
R_{po}	radius of the passage downstream of the vanes (ft)
R_{rz}	max. radius of the recirculation zone (in)
S	the swirl number (non-dimensional)
S_{pri}	swirl number of the primary swirler
S_{sec}	swirl number of the secondary swirler
S_{comb}	overall swirl number of a radial-radial swirler
U	axial component of velocity (ft/s)

V_{flow}	airflow velocity vector at a point
VLP	swirler vane loading parameter
$V_{rz\ max}$	maximum axial back flow velocity in the recirculation zone (ft/s)
W	tangential component of velocity (ft/s)
W_p	mass flow through the primary swirler (lbs/s)
W_{rz}	recirculated mass flow (lbs/s)
W_s	mass flow through the secondary swirler (lbs/s)
W_t	total mass flow in the swirler (lb/s)
X_{rz}	furthest upstream point of the recirculation zone (in)
β	radial angle at a point (°)
ϕ_v	swirler vane angle (°)
ϕ_{mw}	mass weighted average angle of the air flow (°)
θ	angle between air flow angle and a radial line (°)
η	turning efficiency of the swirl vanes
ρ	air density (slugs/ft ³)

INTRODUCTION

Gas turbine combustors are required to sustain a flame over a wide range of operating conditions. To accomplish this, most combustor designs create a toroidal flow reversal which entrains and recirculates a portion of the hot combustion products which then mixes and preheats the incoming fuel-air mixture, helping to establish a stable flame. In the past, this recirculation zone was generally created by a combination use of swirling air entering through the combustor dome, and primary dilution air entering through holes in the liner walls. The swirling air was generated by using one or more dome swirlers placed around each fuel nozzle. These swirlers were usually of the axial- or radial-vane-type. More recently, due to the desire for reduced NO_x emissions, combustor designers have been reducing primary zone temperatures by putting a larger percentage of the combustor airflow through the dome

Presented at the International Gas Turbine and Aeroengine Congress and Exposition
Cincinnati, Ohio – May 24–27, 1993

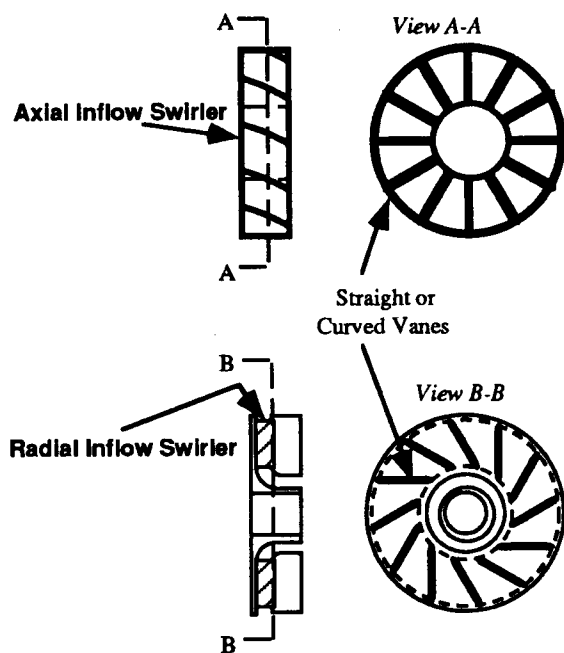


FIGURE 1 - TYPICAL SWIRLER DESIGNS

swirlers. This increased swirler airflow has enhanced the impact of swirler design on combustor performance and thus created a need for a better understanding of swirler-induced recirculation and the design parameters that affect it.

Air is usually swirled through the use of axial vanes, radial vanes, angled holes, or some combination of these methods. Modern swirlers (i.e., airblast, air-assist type) are designed not only to help distribute the fuel, but also to aid in the atomization of the fuel through the use of pre-filming surfaces. There exists a large variety of swirler/fuel injector/liquid-filming-surface each with its own performance advantage. This work describes the effect of swirler geometry on the combustor recirculation zone (and thus performance) with particular emphasis on the radial inflow designs.

BACKGROUND

In a typical aircraft engine combustor, air from the compressor enters the combustor through the swirler at the front of the combustor dome and through dilution holes along the combustor liner. The liquid fuel is injected at the swirl-vane centerline and distributed by the swirling air into the combustion region. When swirling air enters the combustion chamber, its tangential momentum usually causes it to flow radially outward from the swirler centerline, creating a lower static pressure region at the centerline. If the swirl is sufficient, a toroidal flow reversal occurs. This flow reversal is usually desirable and generally causes improvements in flame stability and combustor performance.

Swirling flow is generally produced with axial or radial vanes (see Figure 1). Radial vane designs, although they require a downstream passage to turn the flow in an axial direction, are usually easier to manufacture due to a simpler vane geometry. The vane geometry of radial swirlers also allows them to be more easily modified when changes in airflow are required (e.g. a simple reduction or increase in the vane height is usually sufficient). The downstream passage in radial swirler designs also reduces the effect of aerodynamic wakes (and possible flame anchoring) at the trailing edge of the vanes since they are further away from the combustion zone. Recent experiments by various workers indicate that radial swirlers do not, of themselves, introduce any performance or emissions penalties (Shultz, 1974; Alkabeeb & Andrews, 1988, 1989, 1990, 1991).

THE SWIRL NUMBER

The degree of swirl in a swirling flow was first characterized by Beer & Chigier (1972) through the introduction of the *swirl number*, S . The swirl number is based on the assumption that the flux of axial momentum, G_x , and the axial flux of angular momentum, G_t , are conserved in any *cross section* of a swirling jet. These quantities can be written as:

$$S = \frac{G_t}{G_x R} \quad (1)$$

such that:

$$G_x = \int_0^R U \rho U 2\pi r dr + \int_0^R p 2\pi r dr \quad (2)$$

$$G_t = \int_0^R (W_r) \rho U 2\pi r dr \quad (3)$$

The swirl number is thus non-dimensional and increases as the tangential component of velocity increases. Generally, the swirl number must be above 0.5 to 0.6 before a recirculation zone is established, although this depends on the swirler and downstream geometry. An increase in swirl number leads to an increase in the recirculation zone size and thus, an increase in the recirculated mass flow. More recently, due to the advent of laser diagnostics and computer modeling, the definition of the swirl number has been extended to include the effect of turbulent momentum (Gupta, 1984).

The generic form of the Swirl Number definition makes it very difficult to compare data obtained from different sources or with different geometry. Accurate velocity profiles are often difficult to obtain, and actual integrations of the velocity profiles are often replaced by empirical relationships, and the pressure term (in equation 2) is only rarely included in the calculation. This raises the following questions:

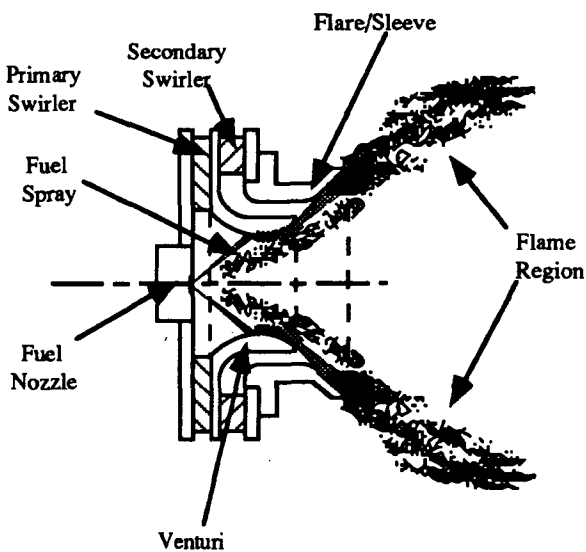


FIGURE 2 - RADIAL RADIAL SWIRLER GEOMETRY

- i) In real systems (as shown in Figure 2), two or three swirlers are often used together. Should the overall swirl number be calculated from the combined velocity profile or an average of the swirl number from each swirler?
- ii) If two swirlers are counter-rotating, do the swirl numbers cancel each other or are they additive?
- iii) In radial swirler systems, the recirculation zone sometimes extends upstream into the swirler passage. How should this recirculated air be handled in the calculation?

Clearly, even if accurate velocity profiles exist, the calculation of the swirl number is not always straightforward.

THE TEST HARDWARE

The radial-radial swirler geometry of particular interest to this work is illustrated in Figure 2. The design consists of two radial swirlers separated by a venturi. Liquid fuel is injected through a simplex- or duplex-type pressure atomizer into the primary swirler air stream. The small droplets are swept downstream with the primary swirler airflow while the large droplets impinge on the venturi surface. The fuel sheet on the venturi flows downstream and is further atomized off the edge of the venturi in the mixing region of the primary and secondary swirler flows. These swirler flows are usually counter-rotating to maximize the turbulence intensity in the shear zone and thus improving atomization for combustion downstream of the "swirl cup" exit. The secondary passage is flared outward downstream of the venturi to help distribute the fuel radially. The swirler vanes are straight for the development stages of the swirl cup design and are curved to improve the aerodynamic performance once the desired swirl

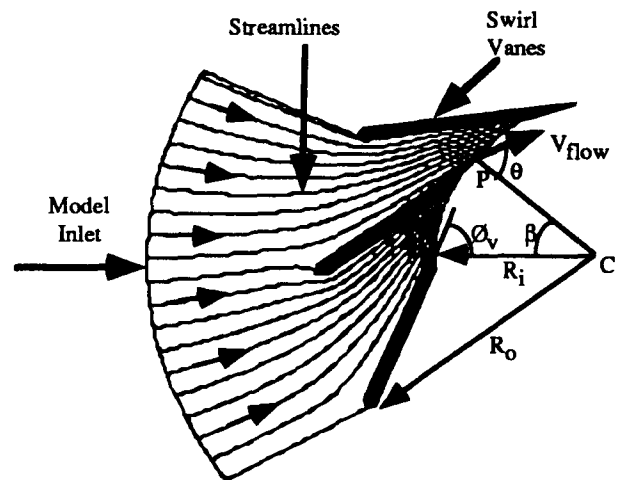


FIGURE 3 - SWIRL VANE FINITE ELEMENT MODEL

cup performance has been achieved. In all the calculations and experiments, no account of the liquid fuel was made and it was assumed that the fuel flow does not significantly affect the swirl cup aerodynamics. Strong support for this assumption was recently obtained through phase doppler particle analyzer measurements performed on similar designs at the University of California (Wang et al., 1991).

Whenever possible, the modeling results were verified using a "variable swirler" test rig. This rig was designed to be modular. The separate parts of the swirl cup, primary swirler, venturi, secondary swirler and flare/sleeve, can be changed independently, are self-centering, and are all aft mounted. The air flow and swirl angle are varied by using primary and secondary swirlers of different vane heights and angles. Various venturis were used to evaluate venturi length and throat radius effects on airflow. The downstream dome height could be set at 2.2", 3.3" or 4.7". Airflow measurements were performed at 8", 16", and 24" H₂O across the swirl cup (~ 2%, 4%, and 6% pressure drop across the cup). With air flowing through the cup, the downstream flow field could be evaluated using a thin-thread tuft on the end of a probe. Thus, the gross characteristics of the flow field and the size of the recirculation zone could be evaluated.

A VANE TURNING PARAMETER

To evaluate the turning effectiveness (sometimes called "vane solidity") of radial swirl vanes, a finite element computer model of the swirl vanes was developed by taking a 3-vane sector of the radial swirler. Figure 3 illustrates the swirl vane finite element model. A computational fluid dynamics code (CONCERT2D) developed at GE Aircraft Engines was used. This code calculates a steady-state solution of the Navier-Stokes equations in a non-orthogonal body-fitted coordinate system in a viscous flow field using the basic k-ε turbulence model (Shyy & Braaten, 1986). In this work,

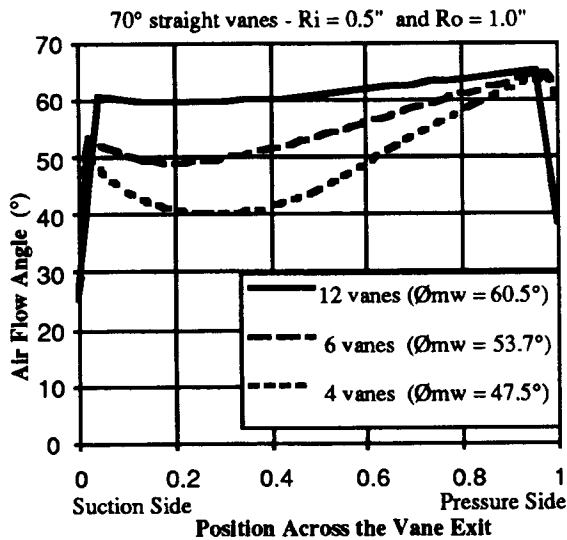


FIGURE 4 - EFFECT OF THE NUMBER OF VANES

the flow velocity was specified at the upstream inlet, periodic boundaries were used along the sides of the domain, and the model used conventional extrapolation at the flow exit. The stream line solution to one vane configuration is also given in Figure 3. Since the finite element grid is structured such that the flow field exit is at the inner radius of the vanes, an analysis of the model-exit velocity vectors permits the evaluation of the turning effectiveness of the vanes. Figure 4 is a plot of the angle of the airflow between two 70° vanes. As can be seen, the airflow never attains an angle of 70°. To allow comparison of different designs, the mass weighted average angle of the flow $\bar{\phi}_{mw}$ was calculated for many different configurations.

An analysis of these data lead to establishment of a radial swirler Vane Loading Parameter (VLP) based on the turbine nozzle loading parameter developed by Zweifel (1945). If one assumes that the dynamic pressure in a vane passage is much smaller at the vane inlet than at the exit, the Zweifel parameter, in terms of radial swirler vane geometry, takes the form shown in equation 4. A plot of this VLP as a function of the mass weighted turning angle $\bar{\phi}_{mw}$ of the air flow is given in Figure 5. As can be seen, for low vane loading the vane turns the flow above 90% efficiency. When the VLP increases above 1.0, the turning efficiency decreases dramatically. Thus, the following criterion for radial swirl vanes was established:

For good aerodynamic performance:

$$VLP = \frac{2 B_p \sin(\bar{\phi}_v)}{R_o - R_i} < 1.0 \quad (4)$$

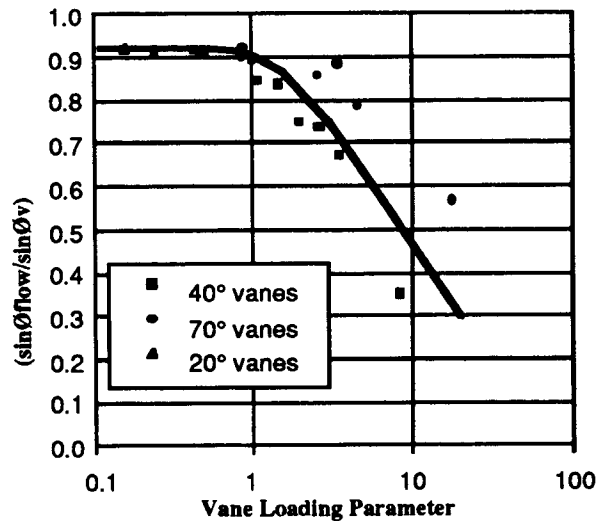


FIGURE 5 - TURNING EFFICIENCY VS. VLP

SWIRLER DESIGN PARAMETERS WHICH AFFECT RECIRCULATION

To evaluate the aerodynamic characteristics of radial swirlers, an axisymmetric finite element swirler model was developed as shown in Figure 6. The inlet conditions were defined based on the results of the vane model. The inlet velocity profiles were defined and the code computed the flow field using conventional extrapolation at the downstream exit plane. The model allowed the evaluation of a variety of swirl cup design parameters. The effects of the design changes were compared as a function of the recirculation zone characteristics shown in Figure 7. The first design parameter of interest is the swirl angle of the vanes. The swirl angle must be high enough to generate good recirculation, but an increase in vane angle causes a decrease in the discharge coefficient C_d of the swirler. This is compensated for by increasing the vane height and consequently the size and weight of the swirler, which is usually undesirable for aviation gas turbine applications. The primary swirler vane-angle effects on the recirculation zone (no secondary swirler air flow and a straight non-venturi passage) are summarized in Table 1 and Figure 8. As the vane-angle is increased the swirl number increases. For this configuration, a 55° vane angle ($S = 0.85$) was necessary for a recirculation zone to be established. Once a recirculation zone is established, an increase in vane angle causes an increase in the recirculation velocities and length. It also moves the recirculation zone further upstream. Thus, it seems that for good recirculation in a radial swirler the vane-angle should be greater than 60°.

When the primary swirler flow was measured in the test rig, the "tufting" showed that recirculation was easier to establish. Three different vane angles were tested (20°, 40°, and 70°) and only the 20° vanes showed no recirculation zone. The tuft test also showed that the 70° vanes had a recirculation zone that

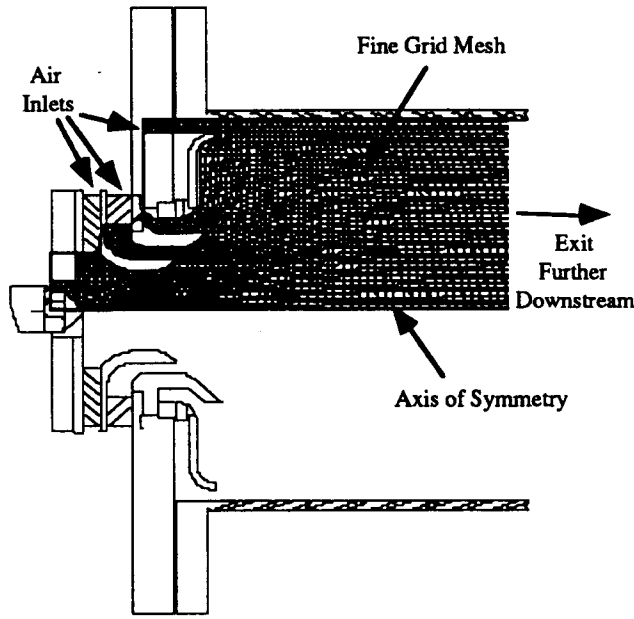


FIGURE 6 - SCHEMATIC OF THE SWIRLER MODEL

was approximately 2" longer than that of the 40° vanes. It is believed that the difference is due to the venturi-shaped passage used in the test rig. To evaluate this the model grid was modified to have a venturi shaped passage as shown in Figure 6, keeping the minimum diameter at 0.34". As seen in Table 2, the venturi caused a recirculation zone to be established. Thus the shape of the downstream passage can have a significant impact on the existence and size of the recirculation zone. The flared out section of the venturi design allows the flow to gain a radial component of velocity inside the venturi passage, thus allowing the flow to turn outward into the dome more easily. Therefore, the swirl number (S) alone is not sufficient to determine the recirculation zone characteristics.

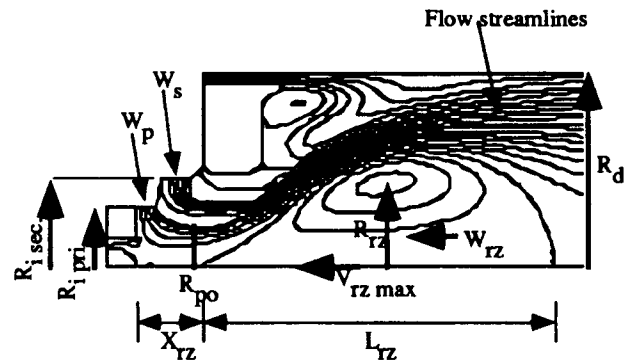


FIGURE 7 - PARAMETERS OF INTEREST

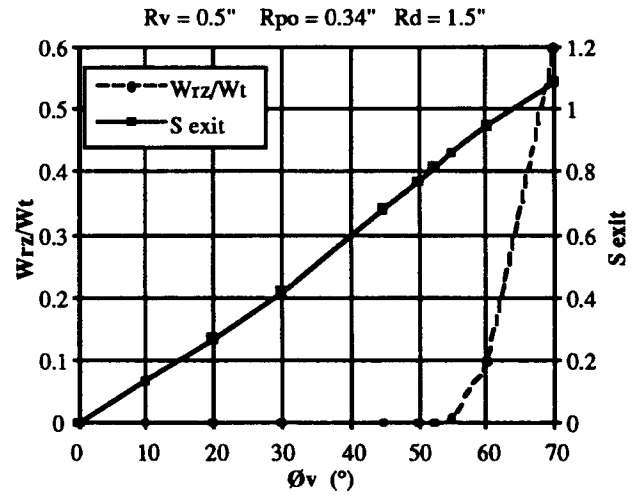


FIGURE 8 - VANE ANGLE EFFECT

TABLE 1 - VANE ANGLE EFFECTS
(Model Results)

($R_i = 0.5"$, straight passage $R_{po} = 0.34"$, $R_d = 1.5"$)

θ_v (°)	$V_{rz \max}$ ft/s	R_{rz} in.	X_{rz} in.	L_{rz} in.	W_{rz}/W_t	S
50	0	0	-	-	0	0.77
52.5	0	0	-	-	0	0.81
55	-9	0.2	2.0	1.0	0.01	0.86
60	-43	0.6	0.98	2.6	0.10	0.95
70	-103	0.85	0.61	3.4	0.60	1.10

TABLE 2 - PASSAGE GEOMETRY EFFECT
(Model results)

($R_i = 0.5"$, $R_{po} = 0.34"$, $R_d = 1.5"$, 40° vanes)

passage type	$V_{rz \max}$ ft/s	R_{rz} in.	X_{rz} in.	L_{rz} in.	W_{rz}/W_t	S
straight	0	0	-	0	0	0.51
venturi	-25	1.05	0.85	1.57	0.65	0.51

TABLE 3 - EFFECT OF DOUBLING THE FLOW

(Model results)

($R_i = 0.5"$, straight passage $R_{po} = 0.34"$, $R_d = 1.5"$, 70° vanes)

Config	V_{rz} max ft/s	R_{rz} in.	X_{rz} in.	L_{rz} in.	W_{rz}/W_t	S
baseline	-90	0.67	0.67	1.75	0.40	1.11
increased pressure drop	-180	0.67	0.67	1.85	0.40	1.10
increased vane height	-10	0.2	1.2	0.4	0.05	0.89

In a combustor development program, the airflow through the swirler is often varied to help optimize the burner performance. One way to vary the airflow is to vary the pressure drop across the swirler; however this is generally not acceptable. Varying the pressure drop requires a change in the complete engine cycle. Thus, airflow changes are usually accomplished through a change in the effective area of the swirler itself. For radial swirlers, this is usually done by changing in the vane height. The problem with changes in airflow is that more or less flow passes through the downstream passage and the effect of this on swirl and recirculation is unclear. To study this effect, three different cases were evaluated with the model:

- a) a baseline design;
- b) an increased pressure drop case with double the airflow;
- c) an increased vane height design with double the airflow.

The results for these three cases are summarized in Table 3.

As can be seen in Table 3, a change in flow due to a change in pressure drop has little or no effect on the dimensions of the recirculation zone, however it doubles the maximum back flow velocity. This indicates that an increase in pressure drop increases both the tangential and axial momentum flux, but does not significantly affect the swirl number. We also see that the increase via a change in vane height causes a significant change in the recirculation zone. The increased vane airflow also goes through the downstream passage which has not increased in size. Orifice-in-series effects cause the passage to "throttle" the flow to a greater degree, reducing the tangential momentum flux. Thus, the swirl number is reduced and the recirculation zone is almost eliminated. Again, the downstream passage has a strong impact on the recirculation zone, even if the swirl vanes are thought to be similar. Therefore, in a real application, if the airflow is to be varied (while maintaining the recirculation zone intensity) the dimensions of the venturi or secondary passage should be adjusted accordingly.

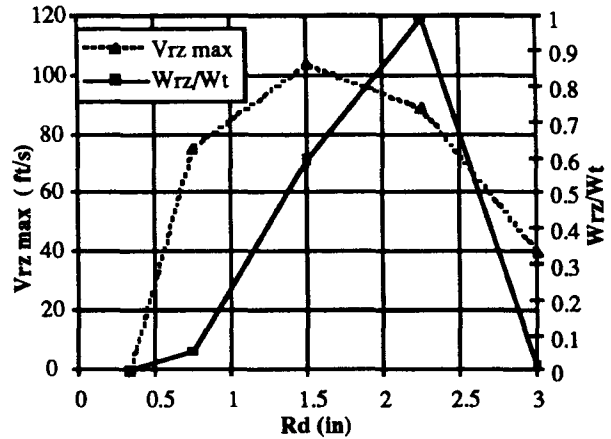


FIGURE 9 - COMBUSTOR DOME RADIUS EFFECT

Another parameter of interest in swirl cup design is the effect of dome height on recirculation. The geometry of the single-swirler model was varied to estimate the effect of dome height on recirculation. (Since the model is axisymmetric, the dome height here is termed "Dome Radius", R_d .) The vane angle 70° , vane radius $0.5"$, and straight passage radius $0.34"$ were held constant while the dome radius, R_d , was varied. The results are summarized in Figure 9. The somewhat surprising result shown in the figure indicates that there is an optimum ratio of (R_d/R_{po}) which maximizes the recirculation zone. In this design, the maximum occurs when R_d/R_{po} is between 4.5 and 6.6. Tufting tests with a variety of swirl cup designs confirmed this trend. Although actual velocities and mass flows could not be measured, when the dome height was set at $3.3"$, all the cups had measured recirculation zones between $1"$ and $4"$ long and approximately $2"$ in diameter. When the combustor liners were removed (i.e., infinite dome height), most of the designs had no detectable recirculation zone. Those that did maintained a recirculation zone less than $0.5"$ in length and diameter.

This height effect is of importance to the combustion engineer. To build smaller and lighter combustors with lower emissions, dome heights have generally been reduced. At the same time swirler airflow has increased. Thus, the ratio, $R_d/R_{swirler\ exit}$, has been steadily decreasing; this indicates that combustor designers will have difficulty in maintaining recirculated mass flows at high levels unless there is a parallel increase in swirl number. Otherwise, a decrease in flame stability and combustion efficiency (and thus an increase in CO and UHC emissions) will probably result. Time limitations did not allow for a systematic study of this effect; however, future work will attempt a more detailed characterization of this phenomenon.

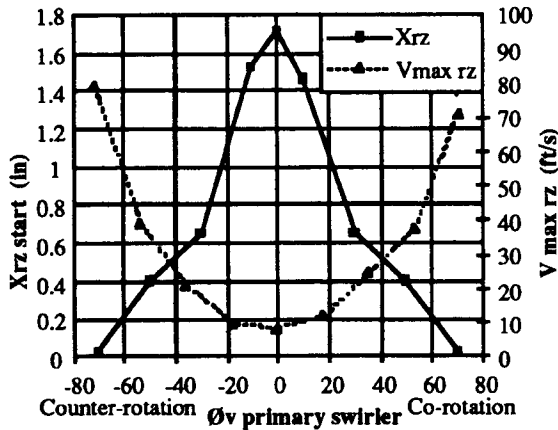


FIGURE 10 - PRIMARY VANE ANGLE EFFECTS

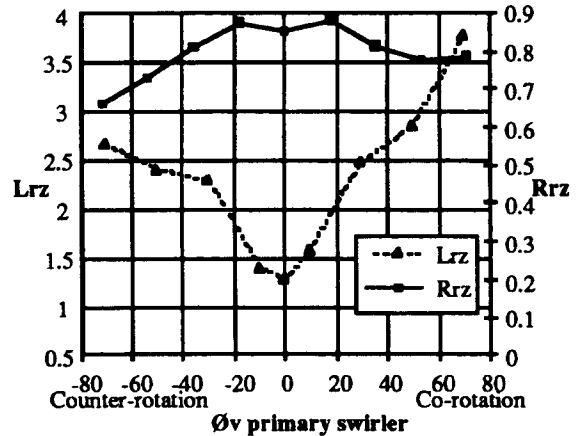


FIGURE 11 - PRIMARY VANE ANGLE EFFECTS

CO-ANNULAR SWIRLERS

Most radial-radial swirl cup designs used in engine applications are counter-rotating. It is believed that counter-rotation causes a higher turbulence intensity in the shear region at the trailing edge of the venturi, thus improving atomization. However little work has been done to determine the effect of counter-rotation on the recirculation zone. The definition of the swirl number would lead one to believe that recirculation would be significantly reduced by counter-rotation. Yet, laser doppler anemometry work performed by Mehta et al. (1989) indicates that counter-rotation creates a larger recirculation zone. The swirl cup model and tufting tests performed here support this surprising result. In the model, while keeping the secondary vane angle fixed at 70° , the primary vane angle was varied from -70° (counter-rotation) to $+70^\circ$ (co-rotation); the results are illustrated in Figures 10 through 13. As can be seen, the model shows only slight differences between the characteristics of the recirculation zone for co- and counter-rotation. The maximum back flow velocity and the beginning point of the recirculation zone are almost perfectly symmetric about the 0° line (Figure 10). At high primary vane angles, co-rotation shows a slightly larger recirculation zone (Figure 11). This is probably caused by the reduction in tangential velocity in the counter-rotation shear region which reduces the tendency to flow radially, reducing the recirculation zone size. Yet, at these same conditions we see that counter-rotation has a greater recirculated mass flow (Figure 12). Again, this is probably due to the lower swirl air in the counter-rotation shear region which recirculates more easily. The model thus shows that co- and counterrotating designs generate similar recirculation zones with differences attributable to the small amount of "de-swirled" air in the counter-rotation shear region.

Tufting tests were used to evaluate this effect. By moving the tuft in the flow field the dimensions of the recirculation zone could be estimated with an accuracy of approximately ± 0.5 ". The results are summarized in Table 4. As shown, no significant difference could be detected between the co- and

counter-rotation. Table 4 also indicates that an increase in the primary vane angle causes an increase in the size of the recirculation.

The swirl numbers calculated by the model are plotted in Figure 13. The values of S_{primary} are plotted as absolute values to simplify the interpretation. As seen, the swirl number calculated from the combined flow field does not satisfactorily represent the trends established in Figures 10 through 12 and Table 4. Thus, it becomes obvious that a different approach must be used to calculate the swirl number for co-annular swirlers. Another parameter of interest in co-annular swirlers is the mass flow split between the primary and secondary swirler. Often, if the swirler airflow is to be varied, the simplest and least expensive approach is to vary the vane height of either the primary or the secondary swirler. As seen from the tufting tests described in Table 4, an increase in the mass flow ratio W_s/W_p caused an increase in the recirculation zone size. This is probably due to the fact that the secondary vane angle is higher than the primary vane angle; thus, an increase in the secondary fraction means that more of the flow is turned at a higher angle. Since these designs generally have primary vane angles which are less than the secondary vane angle (to avoid flame anchoring near the fuel nozzle), an increase in secondary mass flow fraction should result in an increase in recirculated massflux. This trend was confirmed by the model with a 70° secondary swirler and counterrotating primary swirlers (see Figure 14). It is clear from the figure that if both the primary and secondary swirlers have the same vane angle, then the flow-split effect is negligible.

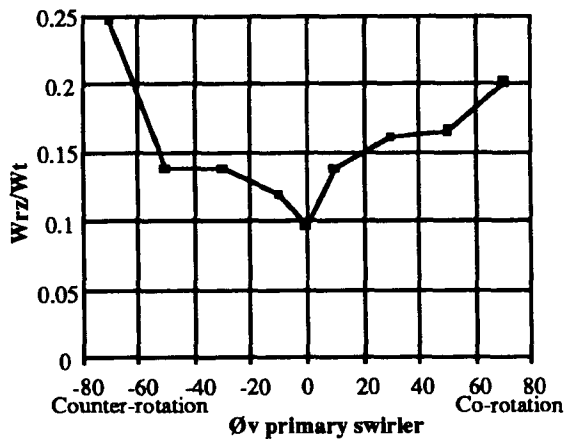


FIGURE 12 - PRIMARY VANE ANGLE EFFECTS

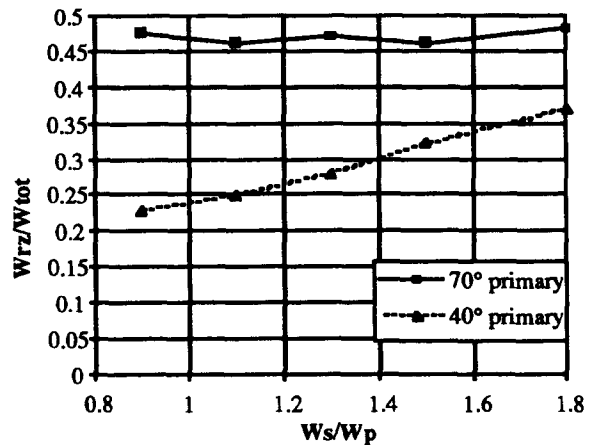


FIGURE 14 - EFFECT OF THE AIR FLOW SPLIT

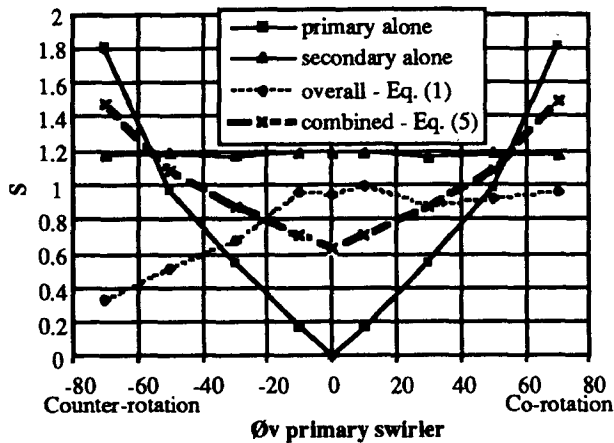


FIGURE 13 - CO-ANNULAR SWIRL NUMBERS

TABLE 4 - CO VS COUNTER ROTATION
(Tufting results)

(constant mass flow, $\phi_{v \text{ sec}} = 70^\circ$ - $\Delta P = 20'' \text{H}_2\text{O}$)

Direction	ϕ_p ($^\circ$)	W_s/W_p	R_{rz} in.	L_{rz} in.
Co	-20	0.93	1.5	2.5
Ctr	+20	0.93	1.5	2.5
Co	-40	0.93	2.3	4.0
Ctr	+40	0.93	2.3	4.0
Co	-40	1.6	2.5	4.5
Ctr	+40	1.6	2.5	4.0

THE SWIRL NUMBER FOR CO-ANNULAR FLOWS

The two previous sections suggest the following equation for the swirl number of co-annular designs.

$$S_{\text{comb}} = \left| \frac{W_p}{W_t} S_{\text{pri}} \right| + \left| \frac{W_s}{W_t} S_{\text{sec}} \right| \quad (5)$$

Equation 5 states that the swirl number for concentric, co-annular designs should be equal to the mass weighted average of the absolute value of the swirl number of the individual swirlers. This calculated value is plotted in Figure 13 (see S_{mw}). This mass weighted swirl number is definitely a better representation of the trends seen in Figures 10 through 12. Future diagnostic work with these swirl cup designs as well as additional modeling should help to confirm the accuracy of Equation 5 in predicting recirculation zone trends.

CONCLUSIONS

The swirl cup recirculation zone characteristics investigated here are by no means an exhaustive list of all possible design parameters. Downstream effects such as dome shape and dilution air were not evaluated here due to the axisymmetric nature of the CONCERT2D code. (These effects will hopefully be evaluated in the future using a three-dimensional computational fluid dynamics code.) The main conclusions from this work can be summarized as follows:

- A vane-loading parameter was developed which establishes criteria to ensure good aerodynamic performance in radial-swirl vanes.
- For well-designed radial swirl vanes, it was found that:

$$\frac{\sin \phi_{\text{flow}}}{\sin \phi_v} \sim 0.9.$$
- It was shown that the swirl number is only indicative of trends for recirculation and that actual recirculated mass

flows are strongly influenced by the geometry downstream of the swirler.

- d) It was determined that there is very little difference between the recirculation zones generated by co- and counterrotating swirl cups and therefore, if the increased shear region of counterrotation gives atomization benefits then they might be preferable.
- e) A method for calculating swirl numbers in co-annular designs was introduced which supports modeling and tufting results.

The above work has outlined some of the aerodynamic issues faced by the swirl cup designer of today's aircraft engines. The results indicate the trends which result from hardware design changes. The optimum type of recirculation zone for minimized emissions or maximize flame stability is still an undefined and important part of the swirl cup puzzle. This investigation will hopefully help to direct us towards this optimization.

REFERENCES

Alkabie, H.S., & Andrews, G.E., "Lean Low NO_x Primary Zones Using Radial Swirlers", ASME Paper 88-GT-245, June 1988.

Alkabie, H.S., & Andrews, G.E., "Ultra Low NO_x Emissions for Gas and Liquid Fuel Using Radial Swirlers", ASME Paper 89-GT-322, June 1989.

Alkabie, H.S., & Andrews, G.E., "Radial Swirlers with Peripheral Fuel Injection for Ultra-Low NO_x Emissions", ASME Paper 90-GT-102, June 1991.

Alkabie, H.S., & Andrews, G.E., "Reduced NO_x Emissions Using Low Radial Swirler Vane Angles", ASME Paper 91-GT-363, June 1991.

Beer, J.M., and Chigier, N.A., Combustion Aerodynamics, Applied Science Publishers, Halstead Press Div., John Wiley & Sons, Inc., New York., 1972, p.100-146.

Gupta, A.K., Lilley, D.G., & Syred, N., Swirl Flows, Abacus Press, Tunbridge Wells, London, 1984.

Lefebvre, A.H., Gas Turbine Combustion, Hemisphere Publishing Corporation, McGraw Hill Book Company, New York, 1983.

Martin, C.A., "Aspects of the Design of Swirlers as used in Fuel Injectors for Gas Turbine Engines", ASME Paper 87-GT-139, 1987.

Mehta, J.M., Hyoun-Woo Shin, Wisler, D.C., "Mean Velocity and Turbulent Flow Field Characteristics Inside an Advanced Combustor Swirl Cup", AIAA paper no. 89-0215, January, 1989.

Schultz, D., F., "Modifications that Improve Performance of a Double Annular Combustor at Simulated Engine Idle Conditions", NASA TM X-3127, 1974.

Shyy, W., and Braaten, M.E., "CONCERT - Cartesian or Natural Coordinates for Elliptic Reacting Flows: A Package of Two- and Three-Dimensional Computer Codes", General Electric Technical Information Series Report 86-CRD-187, Corporate Research and Development Center, 1986.

Wang, H.Y., Sowa, W.A., McDonell, V.G. and Samuelsen, G.S., "Spray Gas-Phase Interaction Downstream of a Co-axial Counter-rotating Dome Swirl Cup", Proceedings of the Fifth International Conference on Liquid Atomization and Spray Systems (ICLASS), pp. 687-694, 1991.

Zweifel, O., "The Spacing of Turbo-Machine Blading Especially with Large Annular Deflection", Brown Boveri Rev. 32. pp. 436-444, 1945.